Temperature and pressure shift of the Cs clock transition in the presence of buffer gases: Ne, N_2, Ar

Olga Kozlova, Stéphane Guérandel, and Emeric de Clercq
Laboratoire National d'Essai-Systèmes de Référence Temps-Espace, Observatoire de Paris, Unité Mixte de Recherche 8630, CNRS, Université Pierre et Marie Curie, 61 Avenue de l'Observatoire, F-75014 Paris, France

(Received 8 April 2011; published 29 June 2011)

The ground-state hyperfine resonance line of alkali-metal atoms is frequency shifted in the presence of noble or molecular gases. The buffer gases used in vapor-cell atomic clocks thus induce a temperature-dependent shift of the clock transition frequency. We report on measurements of the pressure and temperature dependence of the Cs clock transition frequency in the presence of Ne, Ar, and N_2 buffer gases. The pressure in the sealed glass vapor cells is measured by means of the shift of the Cs D_1 line. We have also investigated the temperature dependence of the optical shift. From these measurements, we infer the pressure and temperature coefficients of the hyperfine frequency shift. It is then possible to predetermine gas mixture ratios that cancel the temperature sensitivity at a given temperature. This prediction is confirmed experimentally for Ar-N_2 mixtures. These results can be useful for improving the long-term frequency stability of Cs vapor-cell clocks.

DOI: 10.1103/PhysRevA.83.062714 PACS number(s): 34.90.+q, 32.10.Fn, 32.30.Bv, 32.70.Jz

I. INTRODUCTION

Hyperfine transitions of atoms are frequency shifted in the presence of buffer gases [1]. It is generally considered that during a collision with an atom or molecule of the buffer gas the hyperfine splitting of alkali-metal atoms is modified by the alteration of the valence electron density at the nucleus [2–6]. This alteration is the result of the competition between attractive long-range Van der Waals interactions and repulsive short-range Pauli exclusion forces. The former decreases the electronic density at the nucleus and reduces the hyperfine splitting, while the latter increases the electronic density at the nucleus and enhances the splitting. The resulting frequency shift depends on the nature of the gas, its density, and temperature [7]. Early experiments [1] showed that for cesium atoms the frequency shift is positive with light gases (He, Ne, N_2), where the Pauli exclusion forces are dominant, unlike the heavy gases (Ar, Kr, Xe), where the frequency shift is negative, mainly due to the Van der Waals interactions. This effect is a density shift, also known as a pressure shift, and is usually measured in Hz/torr. Aside from its theoretical interest, this effect is of prime importance in vapor-cell atomic clocks, where a few tens of torr of buffer gases are added in the cell in order to slow down the diffusion of atoms toward the cell walls and to prevent the Doppler broadening [5]. This motivated extensive studies on alkali-metal atoms, especially in Rb [5,8–11]. The shift can reach kHz/torr and its temperature dependence is of the order of Hz/(torr · K), thus affecting the frequency stability of the clock [5]. This drawback can be minimized, or even canceled at a given temperature, using a mixture of gases with temperature coefficients of opposite signs [5,10]. The achievement of good mixing requires an accurate knowledge of the gas characteristics, which are fairly well known for Rb [5] but no so precisely for Cs. We present here measurements of the Cs clock frequency (ground-state hyperfine transition between ($m_F = 0$) Zeeman sublevels) in the presence of buffer gas. The pressure shift rates and temperature shift rates are reported for three gases: Ne, N_2, and Ar.

There is no straightforward theoretical expression for the collisional shift, the best estimation has been performed for He and it is in qualitative agreement with experimental results [6]. In a limited range of pressure and temperature, it is common practice to approximate it with a linear function of pressure and temperature. However, Bean and Lambert [8] used a fifth-order polynomial to fit the temperature shift over a range of several hundred K. In [12] Dorenburg *et al.* used a pressure second-order polynomial linear in temperature, for fitting their data over a few ktorr range. Gong *et al.* [13] have shown that with heavy gases (Ar, Kr) transient Van der Waals molecules are formed, which leads to a small additional nonlinear pressure shift at low pressures. According to Vanier *et al.* [5,10], in the range of pressure (a few tens of torr) and of temperature variation (a few tens of K) encountered in atomic clock working conditions, a temperature second-order polynomial linear in pressure is sufficient. If we add the quadratic term b of Ref. [12] and the nonlinear term $\Delta^2\nu$ of Ref. [13], the collisional shift can be expressed as

$$\Delta\nu(T) = P_0[\beta + \delta(T - T_0) + \gamma(T - T_0)^2] + \Delta^2\nu + bP_0^2, \quad (1)$$

where T is the cell temperature; P_0 is the buffer-gas pressure in the cell at the reference temperature T_0; and β, δ, and γ are experimental coefficients. Note that in this study the b and $\Delta^2\nu$ terms are small and are considered only for Ar. They are discussed in the corresponding section. For a mixture of gases the shifts of Eq. (1) add linearly. The β, δ, and γ coefficients are of great interest for atomic clock applications because they allow for an estimate of inversion temperatures, where the temperature coefficient falls to zero, and gas mixtures which minimize the frequency shift or the temperature dependence around a fixed temperature value.

The accuracy of the measurements of the coefficients is generally limited by the knowledge of the actual gas pressure in the sealed cells. We show in Sec. II how we can measure the gas pressure using the frequency shift of the D_1 line, in part, due to recently measured coefficients by Pitz *et al.*

[14] and Andalkar *et al.* [15]. For this purpose, we have also measured the temperature dependence of the D_1 line shift. Section III is devoted to the measurement of the clock transition shift and to the derivation of the shift coefficients. This constitutes, to our knowledge, the first determination of the quadratic coefficients γ for cesium. These coefficients are used in Sec. IV to foresee the composition of a N_2-Ar gas mixture canceling the temperature dependence of the hyperfine frequency shift. Experimental results confirm the predicted relationship between the inversion temperature and the buffer-gas composition.

II. PRESSURE MEASUREMENT IN SEALED CELLS

A. Method and experimental setup

The extraction of β, δ, and γ of Eq. (1) from experimental measurements of the clock frequency shift requires the knowledge of the actual buffer-gas pressure in the cell at a given temperature. The pressure at any temperature can then be deduced from the ideal gas law. We make use of sealed cells for this experiment, filled with well-defined pressure before sealing. Unfortunately after the sealing process at high temperature the actual pressure in the cell is unknown and cannot be measured directly. We undertook the measurement of the buffer-gas pressure by means of the frequency shift of an optical transition, the Cs D_1 line. This measurement is based on the laser absorption spectroscopy: the shift of the optical transition is proportional to the buffer-gas pressure, $S = \delta_{\rm op} P$, where S is the frequency shift, P the pressure of the buffer gas, and $\delta_{\rm op}$ the pressure shift rate [14–17].

The experimental setup is shown on Fig. 1. A distributed Bragg reflector (DBR) laser diode, of linewidth about 4 MHz, tuned to Cs D_1 line (895 nm) is used. The diode laser current is slowly modulated in order to scan the frequency over 12 GHz. The laser power is greatly attenuated by neutral-density attenuators to reduce optical pumping effects and saturation. Measured intensities used in this experiment were less than 1 μW/cm^2. The transmissions of the laser beams through the Cs cell and Cs–buffer-gas cell are recorded simultaneously by the photodiodes PD1 and PD2, respectively, as the frequency of the laser is scanned around the transitions. The photodiode signals are recorded on a computer. In order to reject the laser intensity variation (induced by the current modulation) during the frequency scan, both cells are moved out of the beam path and a new scan of the background is recorded. The first scan data are then divided by this background signal. As in Ref. [15], we have noticed that this technique is a more effective means of rejecting the residual modulations than normalization by the background signal recorded on the third photodiode (PD0) [18]. The Cs cell is at room temperature, (22.5 ± 0.5) °C, the temperature of the buffer-gas cell can be regulated to within the ± 0.5 °C level. The cells are placed in the ambient magnetic field; we verified that there was no measurable shift compared to a cell placed in a magnetic shield. The cells are made of Pyrex glass. We have at our disposal four cells filled with Ne, five with N_2, and five with Ar, each filled with different pressures ranging between 15 and 180 torr (see Table II). They have a diameter of ~20 mm and lengths varying between 15 and 50 mm. They have been made by four different providers, labeled F, O, S, T [19] in order to avoid a possible bias due to the manufacturing process.

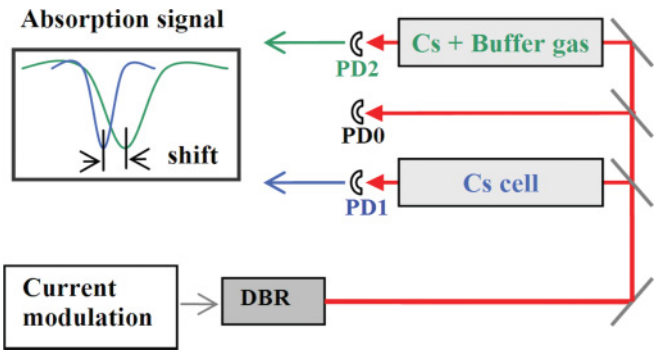

FIG. 1. (Color online) Experimental setup for the pressure measurement. DBR: Distributed Bragg reflector laser diode. PD0, PD1, and PD2: Silicon photodetectors.

Figure 2 shows an example of the absorption spectrum, with the transmitted intensity shown on a logarithmic scale, for the 30-torr N_2 Cs cell. Note that on the x axis the diode current (the frequency) increases (decreases) rightward. The detected transitions are $(F = 3 - F' = 4)$, $(F = 3 - F' = 3)$, $(F = 4 - F' = 4)$, and $(F = 4 - F' = 3)$, where F and F' are the hyperfine numbers of the ground and excited levels, respectively (see inset in the Fig. 2).

The proceedings is as follows. The spectrum of the Cs cell is first fitted with the sum of four independent Voigt profiles to extract the positions x_i of the peak centers. The frequency difference between the peaks is given by the well-known hyperfine structure of the ground and excited states of Cs [20,21]; see inset in Fig. 2. In order to calibrate the x axis in frequency, the center of the transition $(F = 3 - F' = 4)$ is taken as the origin, and the peak frequencies plotted versus the positions x_i are fitted with a third-order polynomial (see an example in Fig. 3), accounting for the nonlinear dependence of the laser frequency versus the current over a wide scan. The absorption spectra of the Cs cell and the Cs–buffer-gas

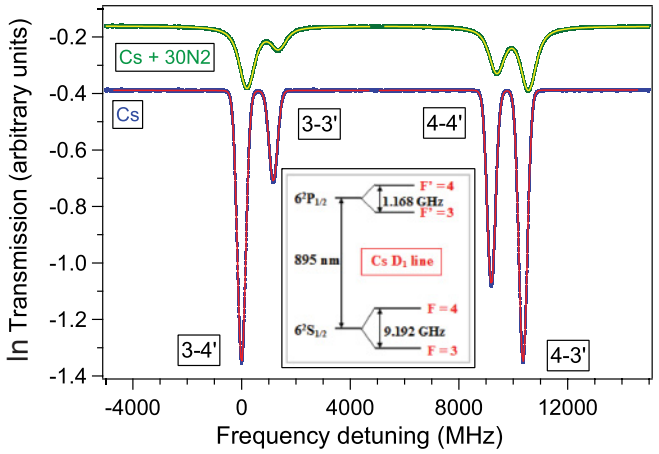

FIG. 2. (Color online) Absorption spectra in Cs and Cs + 30 torr N_2 buffer gas. Dark blue and green curves are the experimental curves for Cs and Cs + N_2 gas cells, respectively. Red and yellow curves are the fits with a sum of Voigt profiles for Cs and Cs + N_2 gas cells, respectively. The inset shows the energy levels involved.

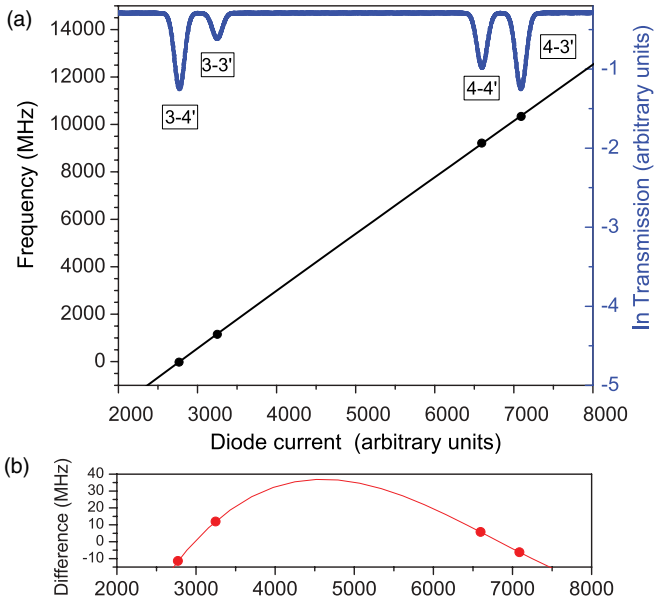

FIG. 3. (Color online) Frequency axis calibration. (a) Dark blue curve is absorption spectrum of the reference Cs cell (right vertical axis). Black dots are the peaks' positions extracted from the fit by a sum of Voigt profiles. The left vertical axis shows the corresponding frequency; the first peak is taken as the origin. (b) Laser frequency versus diode current: difference between a linear fit and a third-order polynomial fit.

cell are then plotted versus frequency. Both spectra are fitted by a sum of four Voigt profiles. The free parameters are the $(F = 3 - F' = 4)$ peak center, the Lorentzian width, the peak amplitudes, and a linear background. The centers of the other peaks are fixed by their distance from the first peak. The Gaussian Doppler width is fixed to the value computed from the cell temperature; we have confirmed with the pure Cs cell that the computed width is in good agreement with the one given by the fitting procedure. The Lorentzian width is not fixed because it is broadened by the collisions and by saturation effects. Finally the optical pressure frequency shift is given by the frequency difference between the fitted $(F = 3 - F' = 4)$ peak centers of both cells.

The fitting process is performed using Igor Pro commercial software. We notice that the peak amplitudes are not in agreement with the theoretical relative line strengths (9, 3, 5, 7) [22] from left to right on the graph. The amplitude ratio is good between two close transitions sharing the same ground-state level ($F = 3$ or $F = 4$), but not between transitions 9 GHz apart. This is explained by the scan method, when the diode current increases, the laser intensity increases and the laser linewidth decreases. Dividing the data by the slope proportional to the laser intensity corrects the first effect but not the second. We have checked with a numerical simulation that the observed relative amplitudes are in agreement with the linewidth variation. We have also verified that at our resolution level the peak center frequencies remained unchanged by this effect.

Finally as the shift of the peak position in the Cs–buffer-gas cell compared that of to the vacuum Cs cell is proportional to the buffer-gas pressure, we can reveal the buffer-gas pressure using the known optical pressure shift coefficients.

B. Temperature dependence of the optical pressure shift coefficients of the Cs D_1 line

Our measurements of the optical transition shift are performed at the temperature 295.5 K. In the most accurate previous reports [14,15] the values of the optical pressure shift rates are given for different temperatures, 294 K or 313–333 K. The temperature behavior of the optical shift at constant density can be written [23,24] as

$$\frac{S_m}{S_r} = \left(\frac{T_m}{T_r}\right)^n, \tag{2}$$

where S_m and S_r are the shifts measured at the temperatures T_m and T_r, respectively, and the value of n is determined by the Cs–buffer-gas interactions and the energy dependence of the cross section. Unfortunately the optical shift temperature dependence is not well documented. In order to determine n, and thus the temperature dependence of the optical pressure shift rates for buffer gas of interest, we carried out the following. For three cells from set (F) (30 torr Ar, 30 torr N_2, and 90 torr Ne) the optical pressure shift was measured for different temperatures in the range 295–323 K. The temperature was controlled to within 0.5 K and the value of the frequency shift was measured with an uncertainty of about 1%. The results are shown in Fig. 4. The data are fitted with Eq. (2). The obtained values of $n = \ln(S)/\ln(T)$ are 0 ± 0.2 (Ne), 0.18 ± 0.03 (N_2), and 0.56 ± 0.07 (Ar) (see Table I).

By knowing the shift dependence, one can derive the optical pressure shift rate dependence for a sealed cell from the ideal gas law $P = n_d kT$, with n_d being the atomic density and k being the Boltzmann constant:

$$\frac{\delta_m}{\delta_r} = \left(\frac{T_m}{T_r}\right)^{n-1}, \tag{3}$$

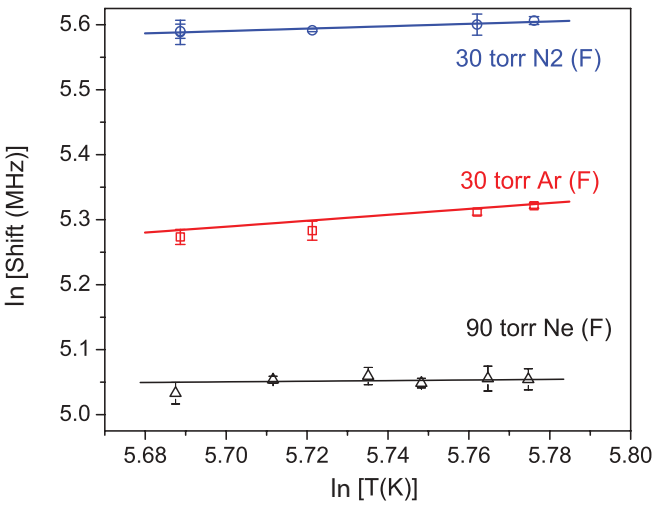

FIG. 4. (Color online) Temperature dependence of the optical pressure shift for Ne, N_2, and Ar buffer gases, in logarithmic units. The slope of each fit is the exponent n of the temperature dependence power law.

TABLE I. Temperature dependence of optical pressure shift and values of optical shift rates for the experiment temperature T_m.

Buffer gas	n this work	n theoretical [23]	δ_r (MHz/torr) at T_r	T_r (K)	δ_m (MHz/torr) at $T_m = 295.5$ K
Ne	0 ± 0.2	0.0	-1.60 ± 0.01 [14]	313	-1.69 ± 0.03
N_2	0.18 ± 0.03		-7.69 ± 0.01 [14]	318	-8.17 ± 0.05
			-7.71 ± 0.01 [14]	323	-8.29 ± 0.05
			-7.41 ± 0.01 [14]	333	-8.17 ± 0.06
			-8.23 ± 0.02 [15]	294	-8.20 ± 0.04
					Mean: -8.21 ± 0.02
Ar	0.56 ± 0.07	0.31	-6.47 ± 0.03 [14]	313	-6.63 ± 0.05

where δ_m and δ_r are the shift rates at the temperatures T_m and T_r, respectively. The most accurate published values of δ_r are listed in Table I with their temperature measurement T_r. The shift rate values scaled to 295.5 K by use of Eq. (3) are listed in the last column.

According to Kielkopf [23], the theoretical n values should be more uncertain for light gases such as He and more reliable for the heavy gases Kr and Xe, due to the introduction in the calculation of an empirical repulsive factor dominated by the attractive interactions for heavy gases. In this case, n should be about 0.3. Romalis *et al.* [24] measured the temperature dependence of Rb lines in presence of He. They observed a discrepancy with the values of Ref. [23] and a difference between values for D_1 and D_2 lines, as Kielkopf does not differentiate both cases. Here we find a better agreement for Ne than for Ar. Further experimental and theoretical studies are needed. Assuming a cross section independent of the velocity distribution Pitz *et al.* [14] estimates $n \sim 0.5$ for N_2. They measured δ_{r,N_2} at three different temperatures: 318, 323, and 333 K (see Table I). Scaled to 295.5 K using Eq. (3) the averaged value is $\delta_{m,N_2} = -8.21 \pm 0.03$, very close to the value of Andalkar *et al.* [15] after scaling at the same temperature: $\delta_{m,N_2} = -8.20 \pm 0.04$. This good agreement gives us confidence in our experimental values of n.

Knowing the optical pressure shift rate [Eq. (2)] at the experimental temperature, we can now infer the pressure in the vapor cells.

C. Results

The buffer-gas pressure P_0 at $T_0 = 273$ K in the sealed cell is calculated by the following equation:

$$P_0 = \frac{S_m}{\delta_m}\frac{T_0}{T_m}, \tag{4}$$

where S_m and δ_m are the measured optical pressure shift and the optical pressure shift rate at the measurement temperature T_m, respectively.

Table II shows the results of the buffer-gas pressure measurement in the cells computed at $T_0 = 273$ K.

III. COLLISIONAL MICROWAVE FREQUENCY SHIFT

A. Experimental setup

The experimental setup used to measure the Cs clock transition frequency is shown in Fig. 5. It is based on the coherent population trapping (CPT) effect [25–27]. The Cs vapor is illuminated by two laser beams tuned to the D_1 line. When the frequency difference of the two lasers exactly matches the ground-state hyperfine splitting, the Cs atoms are placed in a dark state, here a superposition state of the clock states $|F = 3, m = 0\rangle$ and $|F = 4, m = 0\rangle$, uncoupled from the laser fields [26] so that the transmitted light power is increased. The experimental setup uses two original techniques [28]: a so-called double-Λ scheme for the CPT-resonance excitation and a temporal Ramsey interrogation technique, which produces a high contrast and narrow resonances. The fringes' width scales as $1/(2T_R)$, where T_R is the time separation between the light pulses. It has been shown in Ref. [29] that, in the pulsed (Ramsey) regime, the CPT linewidth is not limited by the saturation effect and the light shift dependence is greatly reduced. This method provides a better frequency resolution

TABLE II. Buffer-gas pressure measured in the sealed cells.

Buffer gas	Cell	Optical pressure shift S_m (MHz) at $T_m = 295.5$ K	Buffer-gas pressure (torr) at $T_0 = 273$ K
Ne	90 torr (F)	-155.9 ± 3	85.2 ± 3.3
	90 torr (T)	-147.6 ± 2	81.7 ± 2.7
	180 torr (T)	-269.6 ± 5	147.4 ± 5.6
	90 torr (S)	-128.9 ± 5	70.5 ± 4.1
N_2	30 torr (F)	-263.0 ± 3	29.6 ± 0.4
	30 torr (T)	-237.7 ± 2	26.8 ± 0.3
	60 torr (T)	-472.7 ± 3	53.2 ± 0.5
	30 torr (S)	-197.5 ± 2	22.2 ± 0.3
	23 torr (O)	-172.1 ± 2	19.4 ± 0.3
Ar	30 torr (F)	-195.1 ± 3	27.2 ± 0.6
	30 torr (T)	-173.7 ± 1	24.2 ± 0.3
	60 torr (T)	-367.6 ± 6	51.2 ± 1.2
	30 torr (S)	-138.7 ± 2	19.3 ± 0.4
	15 torr (S)	-79.1 ± 0.5	11.0 ± 0.2

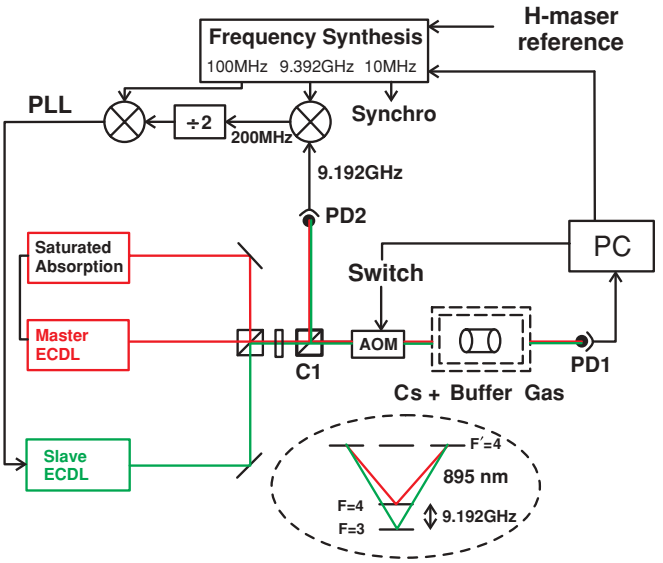

FIG. 5. (Color online) Experimental setup for microwave temperature shift measurements. AOM: Acousto-optic modulator. PD1: Atomic signal photodetector. PD2: Fast silicon photodiode. ECDL: External cavity diode laser. The inset shows the atomic energy levels involved in the double-Λ scheme. PLL: Phase-locked loop. C1: Beam splitter cube.

than the previously reported techniques in Cs (optical pumping [30] or CPT [31] methods).

We use two external cavity diode lasers (ECDL) tuned on the Cs D_1 line at 895 nm. The master laser is frequency locked to the $F = 4$ to $F' = 4$ hyperfine component line by a saturated absorption scheme in an auxiliary vacuum Cs cell. The slave laser is phase locked to the master laser with a frequency offset tunable around 9.192 GHz by comparison with a low-noise synthesized microwave signal [32] driven by a hydrogen maser. For this purpose, the two laser beams are superimposed and detected by a fast photodiode (PD2). The atoms are pumped in the dark state by the two linear and orthogonally polarized laser beams (lin perp lin configuration) propagating parallel to the static magnetic field applied to the Cs–buffer-gas cell. This scheme allows a simultaneous pumping in the dark state with both σ^+ and σ^- polarized lights (double-Λ scheme). The cell is placed inside a nonmagnetic copper cylinder, heated by a coaxial resistive wire. Its temperature, controlled by high-accuracy nonmagnetic thermistors (0.2 K accuracy), is regulated to within the mK level. The axial static magnetic field (about 20 μT) is applied with a solenoid to lift the degeneracy of the Zeeman sublevels. The ensemble is surrounded by two μ-metal magnetic shields. The diameter of the laser beams in the cell is 11 mm and the power is about 0.1 mW. The transmitted power through the cell is detected on the photodiode (PD1).

A pulse sequence is applied, where each pulse is used both for hyperfine coherence preparation and for atomic signal detection. The two laser beams are switched on and off by an acousto-optic modulator (AOM) driven by the computer (PC). The light pulses are 2 ms long spaced $T_R = 4$ ms. A continuous-wave (CW) interrogation is also possible. The frequency measurement is performed by locking the 9.2-GHz synthesizer frequency on the central Ramsey fringe. For this purpose, the synthesizer frequency is square-wave modulated. The absorption signal (PD1) is digitized and computer processed, and the correction signal is applied to the synthesizer. The mean frequency is averaged over a few hours. It is referenced to the hydrogen maser, whose frequency is compared to the Cs clocks of the laboratory.

B. Procedure and results

In order to reveal the temperature dependence of the microwave frequency collisional shift the Cs resonance frequency is measured for a series of temperatures for each Cs–buffer-gas cell. The temperature of the cell is changed in the 25–65 °C range. For each measurement point, the cell temperature is allowed at least 2 h to stabilize. The measured frequencies are corrected for the Zeeman quadratic shift ν_z, using the relationship [33]

$$\nu_z = 8\frac{f_z^2}{\nu_0}, \tag{5}$$

where $2f_z$ is the frequency splitting of the microwave transitions $(F = 3, m = -1) - (F = 4, m = -1)$ and $(F = 3, m = +1) - (F = 4, m = +1)$, and $\nu_0 = 9\,192\,631\,770$ Hz is the frequency of the hyperfine splitting of the unperturbed atom (fixed by definition of the second [20]). The data are also corrected for the light shift [7]. For this purpose, the frequency is measured at different laser power levels for each temperature. The frequency value is then extrapolated to the zero power. We do not apply correction for the spin-exchange frequency shift. It should be negligible [34] since a population imbalance is not created through CPT with equal laser intensities. The frequency is measured with 0.05 and 0.3 Hz final uncertainties in the 25–45 °C and 45–65 °C temperature ranges, respectively. The frequency shift is the difference between corrected frequency and the unperturbed frequency ν_0: $\nu_{\text{shift}} = \nu - \nu_0$.

A typical record of the microwave shift versus the temperature for each buffer gas, Ne, N_2, and Ar, is presented on Figs. 6, 7, and 8.

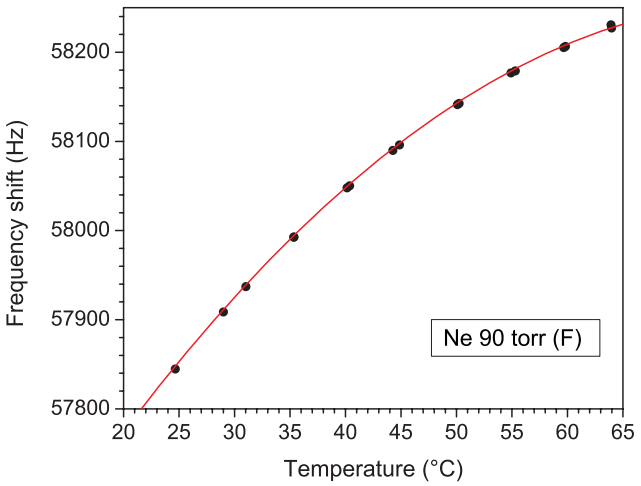

FIG. 6. (Color online) Frequency shift ν_{shift} of the Cs clock transition in the presence of Ne buffer gas. The error bars are within the circles. The solid line is the parabolic fit. Cell Ne 90 torr (F).

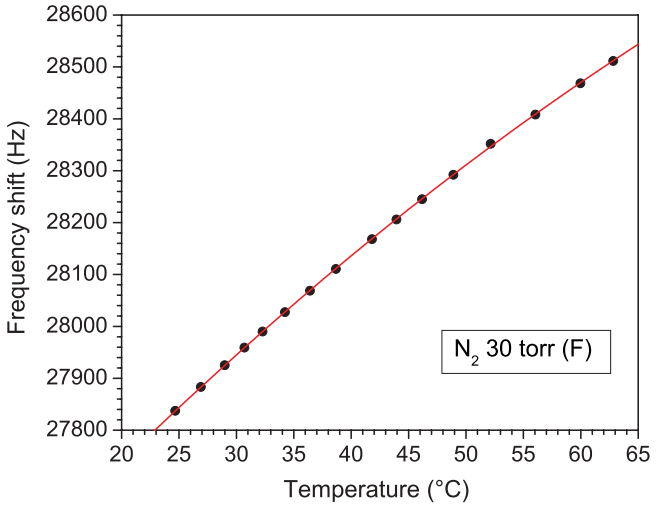

FIG. 7. (Color online) Frequency shift ν_{shift} of the Cs clock transition in the presence of N_2 buffer gas. The error bars are within the circles. The solid line is the parabolic fit. Cell N_2 30 torr (F).

The experimental data are fitted with a second-order polynomial according to Eq. (1). For Ne the b coefficient is zero [12], and the $\Delta^2\nu$ term of Gong *et al.* [13] is unknown. However, this term appears only in heavy gases where Van der Waals molecules can form [13]; it can be here safely neglected. For N_2 the b coefficient is unknown, and the $\Delta^2\nu$ term is zero [13]. We neglect also the b term. So that the β, δ, and γ coefficients of Eq. (1) are obtained for Ne and N_2 by dividing the fitted coefficients by the gas pressure. With Ar the corrective terms bP_0^2 and $\Delta^2\nu$ are weak but must be included, $b = 1$ mHz/torr^2 [12]. The $\Delta^2\nu$ term is [13]

$$\Delta^2\nu = -\left(\frac{1}{2\pi T}\right)\frac{\phi^3}{1+\phi^2}, \tag{6}$$

with $TP^2 = 0.05 \pm 0.01$ s $\cdot$ torr^2 and $\phi P = 3.90 \pm 0.44$ rad $\cdot$ torr for Ar at 35 °C. For the cell with 11 torr Ar $\Delta^2\nu = -15.25$ Hz and is smaller at higher pressure. We also neglect

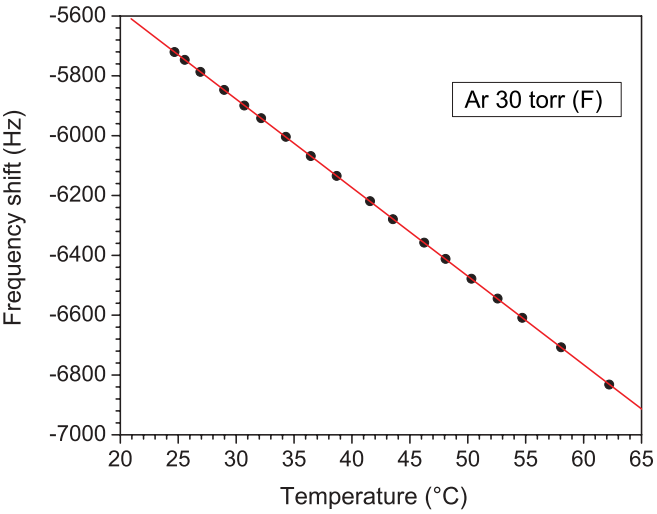

FIG. 8. (Color online) Frequency shift ν_{shift} of the Cs clock transition in the presence of Ar buffer gas. The error bars are within the circles. The solid line is the linear fit. Cell Ar 30 torr (F).

a possible variation of these terms with the temperature. For Ar, the constant coefficient of the fitted polynomial is first corrected for these effects; the collisional coefficients are then computed in the same way. Note, the correction on the β coefficient is of the same order as the error bar. The results are presented in Table III.

In Table IV, previously published and new measured pressure and temperature coefficients for the Cs clock transition are shown. The values of Strumia *et al.* [30] and Beverini *et al.* [9] are referenced to 0 °C and not corrected. The values of Beer and Bernheim [4] were measured between 25 and 28 °C, and those of Dorenburg *et al.* [12] are referenced to 80 °C. The values of Table IV are scaled to 0 °C taking into account our microwave temperature shift coefficients, or with the published coefficient when available (Ar [12]). The accuracy of the present work is still limited by the uncertainty of the buffer-gas pressure. Our values of β coefficients are in good agreement with previous works for nitrogen and argon. For neon the agreement is reasonable. The small discrepancy between present measurement values and our preliminary work [18], carried out on two cells, arises from the inclusion of the temperature dependence of optical shift rates in our model. The δ coefficients are measured with a lower uncertainty compared to previous works. The δ values of Refs. [9,12,30] are smaller than those of the current work, which can be explained for Ne and N_2 because these measurements did not take into account the quadratic term which is negative.

For the first time, the quadratic coefficients γ for N_2 and Ne have been determined. The coefficient γ of Ar is much smaller and we have estimated an upper limit. It is important to notice that gases with a quadratic coefficient exhibit an inversion temperature, where the temperature dependence vanishes, $T_{\text{inv}} = T_0 - \delta/2\gamma$. Ne buffer gas shows a strong quadratic temperature coefficient. The inversion temperature computed from the coefficients of the fitted polynomials for each cell, in order to avoid pressure additional uncertainties, is $T_{\text{inv}} = (79 \pm 3)$ °C, which confirms previous evaluations [18,36]. It makes Ne very attractive for use in the Cs chip scale clocks which need a high working temperature [37–39]. The calculated inversion temperature with N_2 is (164 ± 13) °C, while no inversion temperature can be given for Ar.

One can also cancel the temperature dependence at a chosen temperature by a mixture of gases with temperature coefficients of opposite signs [10,40].

IV. APPLICATION: BUFFER-GAS MIXTURE

It is generally considered [5] that the collisional shifts [Eq. (1)] add linearly in a mixture of buffer gases. For a N_2-Ar mixture, it should then be possible to cancel the temperature dependence of the microwave collisional shift at a given temperature. With P_{Ar} and P_{N_2} being the partial pressures of Ar and N_2 and $r = (P_{\text{Ar}}/P_{N_2})$, the total microwave shift can be written as

$$\begin{aligned}\Delta\nu(T) = P_{N_2}\big[&\big(\beta_{N_2} + r\beta_{\text{Ar}}\big) + \big(\delta_{N_2} + r\delta_{\text{Ar}}\big)(T - T_0)\\ &+ \big(\gamma_{N_2} + r\gamma_{\text{Ar}}\big)(T - T_0)^2\big]\\ &+ \Delta^2\nu(\text{Ar}) + b_{\text{Ar}}\big(rP_{N_2}\big)^2.\end{aligned} \tag{7}$$

TABLE III. Measured pressure coefficient, linear and quadratic temperature coefficients for Cs clock transition in presence of Ne, N_2, and Ar buffer gases.

Buffer gas	Cell	β (Hz/torr)	δ [Hz/(torr K)]	γ [mHz/(torr K^2)]
Ne	90 torr (F)	673.3 ± 29.5	0.264 ± 0.011	-1.70 ± 0.08
	90 torr (T)	692.2 ± 22.7	0.264 ± 0.011	-1.61 ± 0.09
	180 torr (T)	700.6 ± 26.5	0.270 ± 0.014	-1.67 ± 0.11
	90 torr (S)	665.8 ± 33.7	0.272 ± 0.017	-1.80 ± 0.12
	Mean Ne	686.1 ± 13.5	0.266 ± 0.006	-1.68 ± 0.05
N_2	30 torr (F)	921.8 ± 12.8	0.826 ± 0.012	-2.6 ± 0.04
	30 torr (T)	924.6 ± 10.0	0.812 ± 0.010	-2.25 ± 0.05
	60 torr (T)	921.3 ± 8.2	0.811 ± 0.014	-2.33 ± 0.11
	30 torr (S)	919.3 ± 11.6	0.837 ± 0.012	-2.77 ± 0.06
	23 torr (O)	926.8 ± 13.1	0.842 ± 0.017	-2.71 ± 0.11
	Mean N_2	922.5 ± 4.8	0.824 ± 0.006	-2.51 ± 0.03
Ar	30 torr (F)	-183.4 ± 4.2	-1.088 ± 0.025	
	30 torr (T)	-198.4 ± 2.7	-1.148 ± 0.017	
	60 torr (T)	-192.3 ± 4.6	-1.109 ± 0.027	
	30 torr (S)	-195.7 ± 4.3	-1.138 ± 0.026	
	15 torr (S)	-198.1 ± 2.9	-1.166 ± 0.019	
	Mean Ar	-194.4 ± 1.6	-1.138 ± 0.010	0.0 ± 0.3

The temperature dependence of the shift vanishes at the inversion temperature T_{inv} for an r value given by

$$r = -\frac{\delta_{N_2} + 2\gamma_{N_2}(T_{\text{inv}} - T_0)}{\delta_{\text{Ar}} + 2\gamma_{\text{Ar}}(T_{\text{inv}} - T_0)}. \quad (8)$$

From the measured temperature coefficients we get $r = 0.724(12) - 0.00441(9)(T_{\text{inv}} - T_0)$, where the numbers in parentheses are uncertainties.

Several cells were filled in our laboratory with different pressure ratios. Special attention was paid to control the pressure and the cell temperature during the sealing process. We used mixtures of gases supplied by Carbagas (Switzerland) with an uncertainty of about 2% for the ratio of partial pressure to total pressure. The gases' purity was better than 99.999%. Figure 9 shows the experimental temperature dependence of the clock frequency in a cell containing a mixture of Ar and N_2 buffer gases with $r = 0.621 \pm 0.020$ filled with a total pressure of (19.8 ± 0.2) torr at 0 °C. The measured microwave shift is fitted with Eq. (7), where the pressure coefficients and temperature coefficients are fixed and the N_2 pressure and the ratio r are the only free parameters. We find $r = 0.608 \pm 0.0003$ (only statistical fit error given) in agreement with the gas supplier uncertainty. From the fit the total pressure is (19.17 ± 0.004) torr (only statistical fit error), which is different from the filling value, but as said above there can be a discrepancy between the filling pressure and

TABLE IV. Final value and comparison with previous works of the pressure shift coefficients of the Cs clock transition in presence of Ne, N_2, and Ar buffer gases.

Buffer gas	β (Hz/torr)	δ [Hz/(torr K)]	γ [mHz/(torr K^2)]	Ref.
Ne	686 ± 14	0.266 ± 0.006	-1.68 ± 0.05	This work
	657 ± 25	0.254 ± 0.010	-1.59 ± 0.06	[18]
	652 ± 20	0.14 ± 0.10		[9]
	683 ± 14			[35]
	624 ± 5			[12]
	634 ± 5			[4]
N_2	922.5 ± 4.8	0.824 ± 0.006	-2.51 ± 0.03	This work
	924.7 ± 7.0	0.623 ± 0.050		[30]
	888 ± 10			[4]
Ar	-194.4 ± 1.6	-1.138 ± 0.010	0.0 ± 0.3	This work
	-191.4 ± 3.0	-1.05 ± 0.05		[30]
	-193 ± 4	-1.00 ± 0.08		[12]
	-187 ± 10			[4]

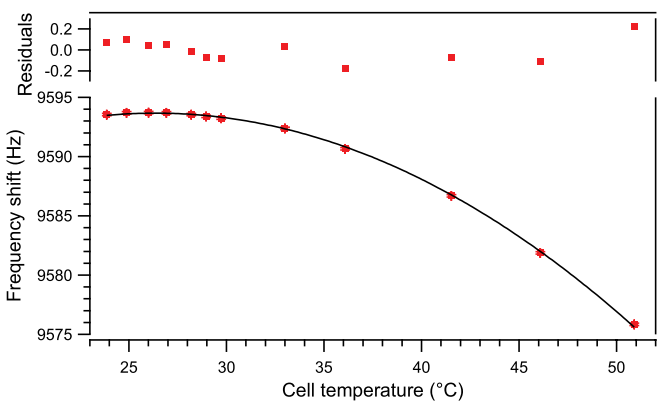

FIG. 9. (Color online) Temperature dependence of the clock frequency shift ν_{shift} in the cell with the buffer-gas mixture Ar-N_2, $r(P_{\text{Ar}}/P_{N_2}) = 0.621 \pm 0.020$ (given by the mixture supplier). Experimental points are fitted with the measured pressure coefficients and temperature coefficients as fixed parameters and with pressure of N_2 and ratio r as free parameters.

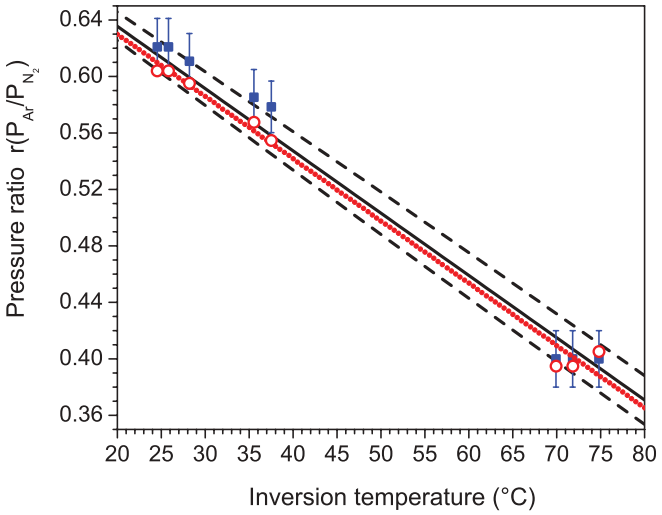

FIG. 10. (Color online) Ar-N_2 pressure ratio versus inversion temperature. Black line: Calculated values from the obtained temperature coefficients. Black dashed lines: 1σ uncertainty for the calculated values. Red open circles and blue squares: Experimentally measured inversion temperatures $T_{\rm inv}$ for 8 cells. For each cell two values of r are plotted. For red open circles r is given by the fit (as explained on the Fig. 9). For blue squares r is given by the gas mixture supplier.

the actual pressure after sealing. The good agreement on the r values supports our coefficients' measurements.

The inversion temperature has been measured on cells filled with different values of r. The results are summarized in Fig. 10 with the expected straight line according to Eq. (8) and the coefficients values of Table IV. The inversion temperature is given in °C. The r plotted values are those given by the fit (as explained for Fig. 9) and by the gas mixture supplier. The agreement is correct taking into account the uncertainty of r. The fitted line expression for the experimental points in the case of values of r given by the fit is $r = 0.718(9) - 0.00441(18)(T_{\rm inv} - T_0)$. The fitted expression for the experimental points in the case of values of r given by the gas mixture supplier is $r = 0.745(17) - 0.00470(33)(T_{\rm inv} - T_0)$.

The close agreement confirms the validity of the measured microwave shift coefficients. This equation and the coefficients values of Table IV can then be a useful guideline for manufacturers of Cs vapor-cell frequency standards.

V. CONCLUSIONS

We have reported here measurements of the frequency shift of the Cs ground-state hyperfine transition in the presence of Ne, N_2, and Ar buffer gases. Measurements have been performed in sealed cells. The actual gas pressure in the cell is measured by means of the frequency shift of the optical D_1 line using known coefficients [14,15]. To apply these coefficients, we have measured the temperature dependence of the optical shift rates (Table I). The pressure and temperature shift rate coefficients of the clock transition are given for Ne, N_2, and Ar buffer gases (Table IV). The microwave pressure shift rates are in agreement with published values. The linear temperature shift rates are reported with a significantly lower uncertainty. The quadratic temperature shift rates with Ne and N_2 gases are reported. An upper limit is obtained for the Ar coefficient. In order to confirm these results we have measured the frequency shift inversion temperature (where the temperature dependence of the microwave frequency shift becomes zero) of cells filled with N_2-Ar mixtures of different composition. Results (Fig. 10) are in good agreement with expected values.

The Cs ground-state hyperfine structure shift in the presence of buffer gases is useful for the study of alkali-metal noble gas interactions and the physics of collisions [3,6,13,41]. It also has applications in vapor-cell atomic clocks, where the use of buffer gases leads to an adverse temperature sensitivity and degrades the long-term frequency stability. Ne shows an inversion temperature around 79 °C and can be used alone in "high" working temperature standards such as microcell clocks [37–39]. At other working temperatures a mixture of gases with opposite sign coefficients can be used. The results reported here allow one to choose the appropriate mixture composition according to the desired working temperature.

ACKNOWLEDGMENTS

We are pleased to acknowledge Pierre Bonnay and Annie Gérard for very careful manufacturing of the Cs cells. We are grateful to Michel Lours and the SYRTE electronic team for their assistance. The help of Jean-Marie Danet is greatly appreciated. We thank John McFerran and François Impens for attentive reading of the manuscript, useful remarks, and corrections. O.K. acknowledges Direction Générale de l'Armement (DGA) for support. This work is partly supported by DGA under Contract No. 2009 34 0052.

[1] M. Arditi and T. R. Carver, Phys. Rev. **112**, 449 (1958).
[2] R. A. Bernheim and L. M. Kohuth, J. Chem. Phys. **50**, 899 (1969).
[3] W. Happer, Rev. Mod. Phys. **44**, 169 (1972).
[4] C. W. Beer and R. A. Bernheim, Phys. Rev. A **13** (1976).
[5] J. Vanier and C. Audoin, *The Quantum Physics of Atomic Frequency Standards* (Hilger, Philadelphia, 1989).
[6] P. J. Oreto, Y. Y. Jau, A. B. Post, N. N. Kuzma, and W. Happer, Phys. Rev. A **69**, 042716 (2004).
[7] M. Arditi and T. R. Carver, Phys. Rev. **124**, 800 (1961).
[8] B. L. Bean and R. H. Lambert, Phys. Rev. A **13**, 492 (1976).
[9] N. Beverini, F. Strumia, and G. Rovera, Opt. Commun. **37**, 394 (1981).
[10] J. Vanier, R. Kunski, N. Cyr, J. Y. Savard, and M. Têtu, J. Appl. Phys. **53**, 5387 (1982).
[11] M. Huang, J. G. Coffer, and J. C. Camparo, Phys. Rev. A **75**, 052717 (2007).
[12] K. Dorenburg, M. Gladisch, and G. zu Pulitz, Z. Phys. A **289**, 145 (1979).
[13] F. Gong, Y. Y. Jau, and W. Happer, Phys. Rev. Lett. **100**, 233002 (2008).

[14] G. A. Pitz, D. E. Wertepny, and G. P. Perram, Phys. Rev. A **80**, 062718 (2009).
[15] A. Andalkar and R. B. Warrington, Phys. Rev. A **65**, 032708 (2002).
[16] E. Bernabeu and J. M. Alvarez, Phys. Rev. A **22**, 2690 (1980).
[17] A. H. Couture, T. B. Clegg, and B. Driehuys, J. Appl. Phys. **104**, 094912 (2008).
[18] O. Kozlova, R. Boudot, S. Guérandel, and E. de Clercq, IEEE Trans. Instrum. Meas. (to be published 2011).
[19] F, Physics Department, Fribourg University, Switzerland; O, Toptica Photonics AG, Germany; S, Sacher Lasertechnik GmbH, Germany; T, Triad Company, USA.
[20] J. Terrien, Metrologia **4**, 41 (1968).
[21] T. Udem, J. Reichert, R. Holzwarth, and T. W. Hänsch, Phys. Rev. Lett. **82**, 3568 (1999).
[22] D. A. Steck [http://steck.us/alkalidata/cesiumnumbers.pdf].
[23] J. F. Kielkopf, J. Phys. B **9**, L547 (1976).
[24] M. V. Romalis, E. Miron, and G. D. Cates, Phys. Rev. A **56**, 4569 (1997).
[25] G. Alzetta, A. Gozzini, L. Moi, and G. Orriols, Nuovo Cimento B **36**, 5 (1976).
[26] E. Arimondo, Prog. Opt. **35**, 257 (1996).
[27] R. Wynands and A. Nagel, Appl. Phys. B **68**, 1 (1999).
[28] T. Zanon, S. Guérandel, E. de Clercq, D. Holleville, N. Dimarcq, and A. Clairon, Phys. Rev. Lett. **94**, 193002 (2005).
[29] N. Castagna, R. Boudot, S. Guérandel, E. de Clercq, N. Dimarcq, and A. Clairon, IEEE Trans. Ultrason. Ferroelectr. Freq. Control **56**, 246 (2009).
[30] F. Strumia, N. Beverini, and A. Moretti, in *Proc. 30th Annu. Symp. Freq. Control* (1976), pp. 468–472.
[31] O. Kozlova, R. Boudot, S. Guérandel, and E. de Clercq, in *Proc. Joint Meeting EFTF IFCS 2009* (2009), pp. 1009–1012.
[32] R. Boudot, S. Guérandel, and E. de Clercq, IEEE Trans. Instrum. Meas. **58**, 3659 (2009).
[33] Y. Koga, Jpn. J. Appl. Phys. **23**, 97 (1984).
[34] S. Micalizio, A. Godone, F. Levi, and J. Vanier, Phys. Rev. A **73**, 033414 (2006).
[35] S. Brandt, A. Nagel, R. Wynands, and D. Meschede, Phys. Rev. A **56**, 1063 (1997).
[36] D. Miletic, P. Dziuban, R. Boudot, M. Hasegawa, R. K. Cutani, G. Mileti, V. Giordano, and C. Gorecki, Electron. Lett. **46**, 1069 (2010).
[37] J. Kitching, S. Knappe, and L. Hollberg, Appl. Phys. Lett. **81**, 553 (2002).
[38] S. Knappe, V. Gerginov, P. D. D. Schwindt, V. Shah, H. G. Robinson, L. Hollberg, and J. Kitching, Opt. Lett. **30**, 2351 (2005).
[39] R. Boudot, P. Dziuban, M. Hasegawa, R. K. Chutani, S. Galliou, V. Giordano, and C. Gorecki, J. Appl. Phys. **109**, 014912 (2011).
[40] R. Boudot, D. Milletic, P. Dziuban, C. Affolderbach, P. Knapkiewicz, J. Dziuban, G. Mileti, V. Giordano, and C. Gorecki, Opt. Express **19**, 3106 (2011).
[41] J. C. Camparo, J. Chem. Phys. **126**, 244310 (2007).